Proposal of an Ultra-Compact Branch-Type Plasmonic Polarization Beam Splitter (PBS)

Ying Huang, Hui Juan Zhang, Saha Soham S., Shiyang Zhu, Tsung-Yang Liow, Minghui Hong, and Patrick Lo G. Q.

***Abstract*—Branch-type polarization beam splitter (PBS) has not been received much attention recently due to its relatively long device-length (~100s μm). In this paper, we proposed a novel design based on the horizontal nanoplasmonic slot waveguide to address this problem. A detailed design principle and procedures to optimize the device parameters are clearly illustrated. Comprehensive numerical analysis is performed to investigate the performance of the devices using the finite-difference time-domain (FDTD) methods. By carefully designing the widths of the branches, we shows that more than 15dB extinction ratio can be achieved, using only 1μm active device length. Proof-of-concept devices are subsequently fabricated in a CMOS-compatible process and characterized, producing results that agree well with the numerical simulation.**

***Index Terms*—Silicon photonics, plasmonics, polarization beam splitter**

I. Introduction

Silicon polarization beam splitter (PBS) has attracted tremendous global research attention recently, driven by the need to address the large structural birefringence in silicon waveguide [1]. Furthermore, integrated PBS provides one of the fundamental building blocks for devices such as coherent receiver [2] and polarization entangled photon sources [3]. There are generally two types of PBS in the silicon platform, directional coupler (DC) type [4]-[6] and branch type [7]-[8]. Unlike the extensive research in the DC-based PBS, the study of branch-type PBS is rather limited. One particular reason could be due to its long device length (typically 100s of μm), which is incompatible with integration due to the precious space on chip.

One the other hand, plasmonic waveguides (PWGs) have been well known for their ability to confine light below the diffraction limit. In addition to the superior device footprint, our recently demonstrated horizontal nanoplasmonic slot waveguide (HNSW) offers advantages of relatively low propagation loss, high coupling efficiency to conventional silicon nanowire and compatibility with the complementary metal-oxide-semiconductor (CMOS) fabrication process [9]. The HNSW platform thus presents the ideal approach to address the long-device length drawback of branch-type PBS from this perspective. In this work, we design an ultra-compact branch-type PBS based on our HNSW. Compare to the existing devices, our device is able to shrink the footprint by 100 times while maintaining excellent performance.

Manuscript received June 6, 2012; revised August 31, 2012.

Y. Huang is with the Institute of Microelectronics, A*STAR (Agency for Science, Technology and Research), 11 Science Park Road, Science Park-II, 117685 Singapore (e-mail: huangy@ime.a-star.edu.sg)

S. Zhang, S. Zhu, S. Liow and Patrick Lo are with the Institute of Microelectronics, A*STAR (Agency for Science, Technology and Research), 11 Science Park Road, Science Park-II, 117685 Singapore.

Soham. S and M. Hong are with Department of Electrical and Computer Engineering, National University of Singapore, Singapore

II. Design and Simulation

A. Design Principle

The PBS is designed using the basic principle developed by W. Burns et al., in which a mode will choose to propagate into the arm with the closest effective refractive index in a branching junction [10]. Identical branches design will result in purely power splitting, as demonstrated in our earlier work [11]. On the other hand, PBS can be realized by utilizing dissimilar branches design. This can be achieved by carefully matching the transverse-electric (TE) or transverse-magnetic (TM) mode refractive index between the input waveguide and desired output waveguide. Mathematically, it can be transformed into a phase matching condition that optimizes the refractive index difference between branches. We define here the effective refractive difference as in Eq. 1, in which nij is the effective refractive index of mode *j* (*j*=TE or TM) in branch #*i* (*i* =1, 2 or 3) and Δn_i^j is the index difference of mode *j* between the input and #*i* output branch. In order to achieve desirable polarization splitting, minimum Δn_2^{TE} and Δn_3^{TM} should be achieved, together with relatively large Δn_2^{TM} and Δn_3^{TE}.

$$\Delta n_2^{TE} = n_1^{TE} - n_2^{TE} \quad (1a)$$

$$\Delta n_2^{TM} = n_1^{TM} - n_2^{TM} \quad (1b)$$

$$\Delta n_3^{TE} = n_1^{TE} - n_3^{TE} \quad (1c)$$

$$\Delta n_3^{TM} = n_1^{TM} - n_3^{TM} \quad (1d)$$

B. Device Design

The schematic diagrams of the proposed HNSW branch-type PBS are illustrated in Fig. 1. The input main branch #1 is the asymmetrical HNSW, as shown in Fig. 1 (b). Simulated modal profiles of the TE and TM mode in the asymmetrical HNSW are illustrated in Fig. 2. The TE mode of the structure is mainly confined in the vertical SiO2 slot region. We then utilize symmetrical HNSW (Fig. 1(c)) for the output waveguide #2 to channel out the TE mode, which also has its TE mode confined in the vertical slots region. Their structure similarities will ensure a simple mapping of

DOI: 10.7763/IJIEE.2012.V2.226

the effective refractive index as well as mode profile. On the other hand, the TM mode of the input waveguide falls entirely in the silicon core. Following the same argument, normal silicon channel waveguide is employed for the TM output branch #3. The devices height (H) and slot width (h) of HNSW are 340nm and 12nm respectively, consistent with our previously fabricated structure [9]. Our analysis shows that they play a less significant role in determining the phase match condition than the width of the three branches. In addition, conservation of waveguide width in the Y-junction implies that the optimization can be reduces to two dimensions (2D), in which $W_1 = W_2 + W_3$. We thus focus on the two waveguide widths (W_2 and W_3) for device optimization, which introduces little fabrication complexity other than the lithography mask re-definition. However, the 2D-optimization is still complex due to the need to look into the four index differences (Δn_i^j).

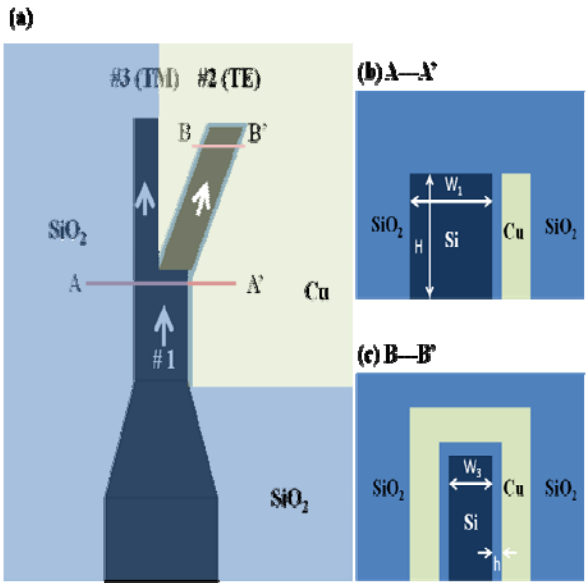

Fig. 1. (a) Schematic diagram of HNSW branch-type PBS, (b) cross section of asymmetrical HNSW in branch #1 and (c) cross section of symmetrical HNSW in branch #2.

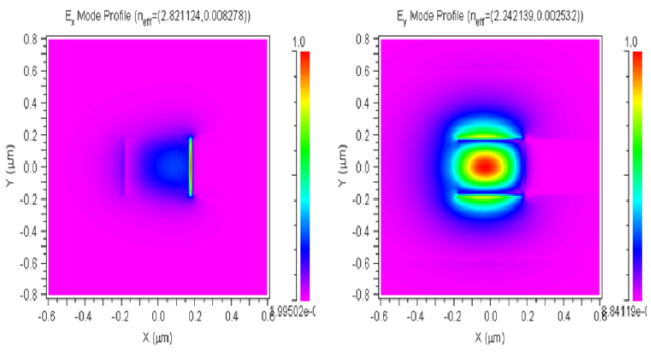

(a) (b)

Fig. 2. The fundamental (a) TE and (b) TM modal profile of the asymmetrical HNSW waveguide at input branch.

Further simplification can be achieved through polarization rejection, in which output branches are designed such that they only support one particular polarization. For the symmetrical HNSW in the output branch #2, the TM mode is cut-off when the waveguide width (W_2) is below 190nm. One can thus eliminate the need to maximize Δn_2^{TM} by design the PBS in this region, rejecting TM mode completely in this branch. Similarly, the TE refractive index drops below that of the surround SiO_2 (1.45) when the silicon waveguide width in output branch #3 decreases under 180nm. This will cause the optical mode to leak into the surrounding cladding, resulting in excessive optical loss. It is thus desirable to operate the PBS below this waveguide width, in which TE mode is virtually not supported in the output branch #3.

By imposing the above mentioned mode rejection criteria, we are now able to reduce the complexity of our optimization to just the Δn_2^{TE} and Δn_3^{TM}. Subsequent search algorithm finds that minimum values occurs when the waveguide dimensions are set to W_2=180nm, W_3 =170nm. The respective refractive indices difference for TE and TM mode between input and desired output branch are 0.09 and 0.39. We note here that Δn_3^{TM} is relatively large, which might generate excess reflection loss in the branching point to deteriorate the performance of the PBS.

C. PBS Performance Simulation

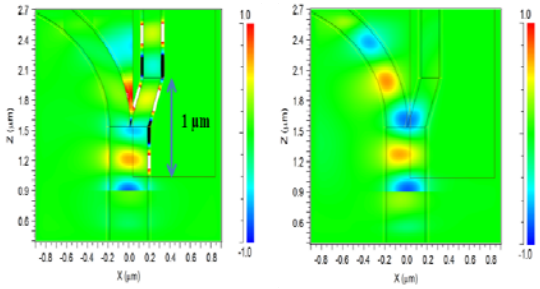

(a) (b)

Fig. 3. Time snap-shots of the electric field strength within the x-z plane (in the middle of the waveguide height) for (a) TE mode and (b) TM mode input. The wavelength is 1550nm.

We subsequently simulate the performance of the optimized branch-type PBS using RSoft FullWave finite difference time domain (FDTD) simulation, as shown in Fig. 3. Distinct branching characteristics are clearly observed for TE- and TM-polarized input light. Incoming TE wave is coupled towards the slot region as it enters the region with copper filling in the input branch. This is subsequently coupled towards the right output branch (#2). A small portion of the light is seemed coupled into the middle of the two branches. We believe this is mainly due to the inability of the left branch (#3) to support TE mode propagation. This portion of light thus corresponding to the power coupled into the left branch, being weakly guide in its cladding. The branching ratio is measured at a relatively low value at 7dB. Due to the leaky nature of the TE mode in the left branch, we believe this will not significantly affect the extinction ratio of the device. Similar behaviour is observed for TM mode input light. A much higher branching ratio is observed as TM mode is virtually cut-off in the right branch. The simulated extinction ratio (ER) is 22dB and 15 dB for the TE and TM mode respectively.

III. Fabrication and Experiments

The devices are fabricated on silicon-on-insulator (SOI) wafers with 340nm top silicon layer and 2μm buried oxide

layer, in a CMOS comparable process that is similar to that used for normal HNSW [9]. One major difference is the windows for metal deposition, which should follow the Cu window as specified in Fig. 1(a) closely. The silicon core of the three branches are first defined in a single lithography process with the help of a 50-nm-thick SiO2 hard mask and photo resist trimming process. An SEM images illustrating the structure of PBS after this stage is shown in Fig. 4. A 50-nm-thick SiN layer and a 1-μm-thick SiO2 layer are then deposited sequentially, followed by the oxide windows opening in the desired region (denoted by the shaped region in Fig. 4). SiN is used as an etch stop layer due to its high etching selectivity with respect to SiO2. This is followed by the formation of a 12nm-thick oxide slot layer through thermal oxidation in the furnace. Copper (Cu) is then deposited onto the whole wafer, followed by a chemical mechanical polishing (Cu-CMP) process to remove the Cu outside of the window. Finally, a 1-μm-thick upper cladding SiO2 is deposition on all wafers, followed by deep trench etching and wafer dicing. The fibre coupling is facilitated by an inverse nano-taper of 200nm-width near the end-facet.

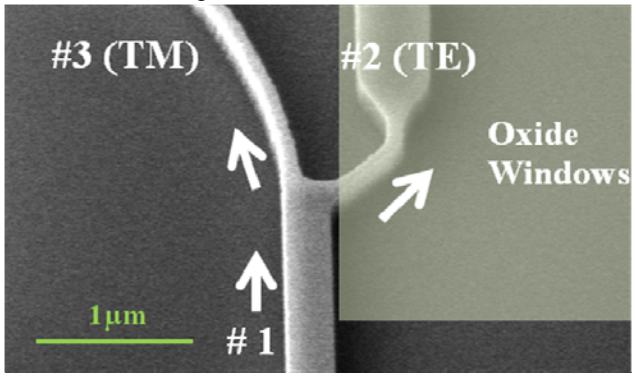

Fig. 4. SEM images of the fabricated HNSW. (Shaped region represents the oxide window opening for Cu deposition)

Experimental characterization of the fabricated proof-of-concept devices is performed. A tunable laser (Ando AQ6317B) is used to characterize the device, capable of scanning the device across the wavelength range from 1530nm to 1610nm. Two identical lensed fibers are used to couple light to and from the silicon waveguide. Two polarization controllers are utilized to align the input polarization to that of the TE mode of the input branch, and adjust the output polarization plane with respect to the polarizer respectively. The output is finally filtered by a polarizer and detected with a power meter (Agilent 8163B). For corresponding measurement of the TM polarization, we just need to rotate the input fiber end and polarizer at the output end by 90o. Significant branching of the TE and TM polarized waves are observed during our experiment. The extinction ratios are measured at 10.2dB and 14.9dB respectively for TE and TM output branches respectively. We noted here that the extinction ratio of the TE is more than 10dB lower than the theoretical predicted value. This could be due to the imperfection in the fabrication process, which results in some Cu being deposited on top of the input waveguide. This might results in excess loss of the TE mode that degrades the TE extinction ratio. Careful control of the overlay between the waveguide layer and oxide windows opening layer should be able to eliminate this problem.

IV. Conclusions

In conclusion, we have designed an ultra-compact broadband PBS based on the horizontal nanoplasmonic slot waveguide. A detailed design principle for branch-type PBS is presented, in which the optimization procedure could be simplified by cutting off the undesirable polarization in the output branch. Comprehensive numerical modelling shows that more than 15dB polarization extinction ratio can be obtained. Proof of concept devices are subsequently fabricated and characterized using our developed CMOS compatible process. More than 10dB extinction ratios are observed for both polarizations, justifying the proposal to be a promising integrated PBS for polarization diversity circuit.

Acknowledgment

This work was supported by Singapore SERC/A*STAR Grant 092-154-0098.

References

[1] J. Zhang, T. Liow, M. Yu, G. Q. Lo, and D. Kwong, "Silicon waveguide based TE mode converter," *Optics Express*, vol. 18, no. 24, pp. 264-270, 2010.

[2] C. Doerr, P. Winzer, Y. Chen, S. Chandrasekhar, M. Sasras, L. Chen, T. Liow, K. Ang, and G. Q. Lo, "Monolithic polarization and phase diversity coherent receiver in silicon," *IEEE J. Lightw. Techno*, vol. 28, no. 4, pp. 520-525, 2010.

[3] K. Harada, H. Takesue, H. Fukuda, T. Tsuchizawa, T. Watanabe, K. Yamada, Y. Tokura, and S. Itabashi, "Frequency and polarization characteristics of correlated photon-pair generation using silicon wire waveguide," *IEEE J. Sel.Top.in Quan. Elec*, vol. 16, no. 1, pp. 325-331, 2010.

[4] H. Fukuda, K. Yamada, T. Watanabe, H. Shinojima, and S. Itabashi, "Ultra small polarization splitter based on silicon wire waveguides," *Optics Express*, vol. 14, no. 25, pp. 12401-408, 2006.

[5] L. Liu, Y. Ding, K. Yvind, and J. Hvam, "Efficient and compact TE-TM polarization converter built on silicon-on-insulator platform with a simple fabrication process," *Optics Letter*, vol. 36, no. 7, pp. 1059-1061, 2011.

[6] D. Dai and J. Bowers, "Novel ultra-short and ultra-broadband polarization beam splitter based on a bent directional coupler," *Optics Express*, vol. 19, no. 19, pp. 614-620, 2011.

[7] R. Ridder, A. Sander, A. Driessen, and J. Fluitman, "An integrated optic adiabatic TE/TM mode splitter on silicon," *J. Lightw. Techno*, vol. 11 no. 11, pp. 1806-1811, 1993.

[8] T. Yamazaki, J. Yamauchi and H. Nakano, "A branch-type TE/TM waveguide splitter using a light guiding metal line," *J. Lightw. Techno*, vol. 25, no. 3, pp. 922-928, 2007.

[9] S. Zhu, T. Liow, G. Q. Lo, and D. L. Kwong, "Fully complementary metal-oxide-semiconductor compatible nanoplasmonic slot waveguides for silicon electronic photonic integrated circuits," *Applied Physics Letters*, vol. 98, no. 2, pp. 021107-1-3. 2011.

[10] W. Burns and A. Milton, "Mode conversion in planar-dielectric separating waveguides," *J. Quan. Elec*, vol. 11, no. 1, pp. 32-39, 1975.

[11] S. Zhu, G. Q. Lo, and D. Kwong, "Nanoplasmonic power splitter based on the horizontal nanoplasmonic slot waveguide," *Applied Physics Letters*, vol. 99, no. 3, pp. 031112-1-3. 2011.